Results in Engineering 24 (2024) 102836

Contents lists available at ScienceDirect

Results in Engineering

journal homepage: www.sciencedirect.com/journal/results-in-engineering

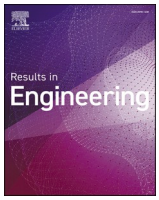

Unravelling flood risk in the Rel River watershed, Gujarat using coupled earth observations, multi criteria decision making and Google Earth Engine

Keval H. Jodhani [a,b], Dhruvesh Patel [a,*], N. Madhavan [c], Nitesh Gupta [b], Sudhir Kumar Singh [d], Upaka Rathnayake [e]

[a] Department of Civil Engineering, School of Technology, Pandit Deendayal Energy University, Gandhinagar, 382426, Gujarat, India
[b] Department of Civil Engineering, Institute of Technology, Nirma University, Ahmedabad, 382481, Gujarat, India
[c] Petroleum Engineering, School of Petroleum Technology, Pandit Deendayal Energy University, Gandhinagar, 382426, Gujarat, India
[d] K. Banerjee Centre of Atmospheric and Ocean Studies, IIDS, Nehru Science Centre, University of Allahabad, Prayagraj, 211002, Uttar Pradesh, India
[e] Department of Civil Engineering and Construction, Faculty of Engineering and Design, Atlantic Technological University, F91 YW50, Sligo, Ireland

ARTICLE INFO

Keywords:
AHP
GEE
Flood hazard
RS-GIS
Flood risk
Rel River

ABSTRACT

Socioeconomic developments, ineffective drainage systems, and insufficient river control, all contribute to significant loss of property and life due to the constant threat of floods. Therefore, controlling flood threats across Rel River, Dhanera, Gujarat has become even more crucial due to floods causing strain throughout the area during monsoon season. The different 52 micro-watersheds were formed across the study region using earth observations for the estimation of flood hazards, vulnerability, and risk. The AHP-MCDM was employed to assign priority rank, weightage, and risk category for each micro watershed. The flood hazard zone was mapped and its vulnerability was characterized in different categories varying from very low to very high. The normalized weights of each factor i.e, hazard indicator (soil, elevation, slope, flow accumulation, rainfall) and vulnerability indicator (LULC, distance from the hospital, population density map) were estimated employing the AHP-MCDM technique whereas LULC along with most of other factors were derived from GEE. The integration of vulnerability and hazard indicators, provides insights into understanding the flood sensitivity, facilitating the preparation of the flood risk map. 20 micro-watersheds were susceptible to high to very high risk and covered an area of 213.15 km^2 whereas 32 micro-watersheds were in the range of very low to moderate category which covers the area of 228.41 km^2. Therefore, the integration of GEE and spectral indices for obtaining various hazard & vulnerability indicators, which were prioritized and ranked using AHP is a unique methodology, facilitating a robust evaluation of flood risk mapping.

1. Introduction

The occurrence of the climate extreme and their severity have been impacted by recent climate changes related to global warming, uncontrollably anthropogenic activity, and sudden changes in land use and land cover [1–5]. Unfortunately, high-magnitude floods have been occurring more frequently over the past 50 years [6]. These patterns disrupt the natural flow of water, river morphology, and hydrological networks, resulting in greater flood likelihood [7–9]. It is increasingly important to assess, control, and chart flood risks to mitigate the damaging impacts of extreme floods caused by shifts in land use patterns [10,11]. Flood risk management demands two vital components: understanding the dangers of floods and implementing methods to mitigate the risks they pose [12]. An important facet of minimizing the impact of flood incidents and accelerating response times is to identify areas with a high risk of flooding and to create thorough maps that address these hazards [12,13]. Modern approaches to flood safety have shifted focus from previously used physical structures to achieving a holistic, management-oriented methodology [14].

This shift in focus has been visible over the last few years. Identifying flood-prone areas and anticipating potential flood scenarios were mapped that have been facilitated with the utilization of geographic information systems (GIS) [15–18]. Understanding of morphological parameters i.e., slope, elevation, flow accumulation, etc., are important in flash flood regions [9]. Therefore, geospatial techniques play a vital

* Corresponding author.
E-mail addresses: jodhanikeval@gmail.com (K.H. Jodhani), dhruvesh.patel@sot.pdpu.ac.in (D. Patel), namadhavan@gmail.com (N. Madhavan), niteshraz@gmail.com (N. Gupta), sudhirinjnu@gmail.com (S.K. Singh), upaka.rathnayake@atu.ie (U. Rathnayake).

https://doi.org/10.1016/j.rineng.2024.102836
Received 3 August 2024; Received in revised form 27 August 2024; Accepted 2 September 2024
Available online 3 September 2024

Abbreviations

AHP	Analytical Hierarchy Process
CHRIPS	Climate Hazards Group Infrared Precipitation with Station
CA	Cluster Analysis
CWC	Centre Water Commission
DEM	Digital Elevation Model
FHI	Flood Hazard Index
FR	Frequency Ratio
FRA	Flood Risk Assessment
FRM	Flood Risk Map
FVI	Flood Vulnerability Index
GEE	Google Earth Engine
GIS	Geographic Information Systems
GOG	Government of Gujarat
IMD	Indian Meteorological Department
LULC	Land Use Land Cover
NASA	National Aeronautics and Space Administration
NBSS & LUP	National Bureau of Soil Survey & Land Use Planning
NIDM	National Institute of Disaster Management
MCDM	Multi-Criteria Decision Making
MSL:	Mean Sea Level
OLI	Operational Land Imager
PCA	Principal Component Analysis
RCC	Reinforced Cement Concrete
RS	Remote Sensing
SRTM	Shuttle Radar Topography Mission
SWDC	State Water Data Center
SYI	Sediment Yield Index
WSA	Weighted Sum Analysis

role in identifying the interrelation among various morphological parameters [19] and determining the flood-prone area [20]. Watershed prioritization is also an application of GIS, which provides the ranking of [20] different sub-watersheds explaining the higher amount of discharge because of high rainfall intensity and erosion [8–16]. Numerous studies are cited in the literature related to flood hazard and risk mapping using remote sensing and GIS [21–25]. In the 1940s and 1950s, Horton and Strahler were the foremost scientists renowned for morphometric analysis. The linear measurement, aerial aspects, and relief aspects of the basin were used to comply with the morphometric analysis [7]. Nowadays, various studies also employ GEE for efficiently handling large amount of the sentinel-1/-2 & landsat 8 satellite datasets for deriving parameter[26–28] and carring out flood risk assessment [29–32].

A development plan of water resource management for the Mayurakshi watershed was planned and conducted a study in which AHP-MCDM and AHP-SYI were used for the prioritization of micro-watersheds under RS and GIS environment [16]. In addition to morphological analysis, AHP-MCDM techniques were also used to identify the most appropriate site for water harvesting structure [33] whereas the combined approach of RULSE, AHP-MCDM, and morphometric analysis was used to identify the soil erosion and susceptibility zones [34]. For a sub-basin of the Kosi River basin [35], suggested FRI for flood risk analysis using the AHP and integrated LULC, topographical, population density & geomorphological parameters. Using GIS with AHP together in flood risk assessment can yield detailed information that is helpful for managing flood risks [36] and flood risk maps with different categories i.e., the very high, very low, medium, high, and low categories can be prepared after the calculation of risk factors using multicriteria analysis [9]. 14 hilly sub-watersheds in the upper Ramganga river basin located in Uttarakhand State, India were prioritized using a weighted sum analysis (WSA) method [37]. Many researchers incorporated the AHP and GIS to assess flood hazards [36–38]. The benefits of using RS data in conjunction with the MCDM method were used to deliver information regarding the hazard assessment in a faster and more cost-effective manner, this is especially true in situations where reliable data are not readily available [39,40].

The evaluation of established flood protection systems relies significantly on flood risk maps and precise mapping of areas susceptible to flooding. In recent times, there has been a shift in focus regarding flood control and intervention methods. This strategy is characterized by the incorporation of hazard calculation research and cost-to-benefit study [41,42]. Globally, numerous studies have concentrated on assessing flood vulnerability and risk using diverse methods. These approaches include CA, PCA, FR, and the integration of the AHP-MCDM approach within a GIS framework [12–19,21–44]. MCDM is an extensively adopted decision-making approach with the goal of selecting the most significant or optimal alternative from a range of potential criteria, as highlighted by Ref. [45]. In current times, numerous researchers have successfully applied MCDM method in studies related to flood-based disaster management, as evidenced by the work of [46]. The attractiveness of this method lies in its simplicity, allowing for the quantification of priorities for multiple qualitative variables [45]. AHP has been widely utilized in FRA due to its reliable, effective, & real-world implementation. AHP addresses multifaceted decision-making scenarios by evaluating the most significant flood causative factors among available alternatives. A systematic assessment process that assigns weight values to all factors, as acknowledged by Ref. [41].

However, very few studies have been steered regarding flood risk mapping using hazard indicators and vulnerability indicators [10]. The indicators were determined by implementing the AHP-MCDM methods with the GIS framework and the LULC map was prepared in the GEE environment using the Random Forest of AI/MLtechnique [47,48]. Therefore, the current study presents a case study of flash floods in a semiarid region, emphasizing the importance of data and watershed characteristics in assessing flood vulnerability, hazard, and risk. The focus is on the Rel River watershed, located in Banaskantha district, Gujarat covers an area of 442 km^2, selected as the study area, which was affected by floods during 2015 and 2017. The main objectives are 1) To understand the basin morphology and their parameters over the 52 micro-watersheds across the river, the ArcHydro tool & ArcGIS 10.3. 2) Implementation of AHP MCDM assign weightage and obtain ranks based on priority levels (very high to very low). 3) To assess the flash flood sensitivity in various micro-watersheds within the study area using the resulting priority rank and integrated priority risk maps. 4) To understand the combination of high-resolution satellite datasets, morphometric analysis, and GIS establishes a robust foundation for exploring each micro-watershed's flash flood hazard potential. Weighted risk mapping played a crucial role in prioritizing the micro-watersheds based on the risk factor. Additionally, a flood risk map was superimposed on the village map, identifying vulnerable villages requiring heightened relief activities. A co-occurrence matrix was prepared to analyse the frequency and patterns of element pairs within the dataset, providing insights into their relationships. This matrix facilitates a deeper understanding of co-occurrence trends [49], essential for the research findings presented in the article. Utilizing a Co-occurrence matrix for flood risk mapping involved analyzing 1816 keywords. Applying a threshold of 12 occurrences, 776 keywords met the criteria, contributing essential insights to the comprehensive development of the flood risk map (Fig. 1).

2. Study area and data used

The Rel River basin originates in the Aravalli Hills near Keshu village of Rajasthan state and flows into Gujarat state. Latitude and longitude

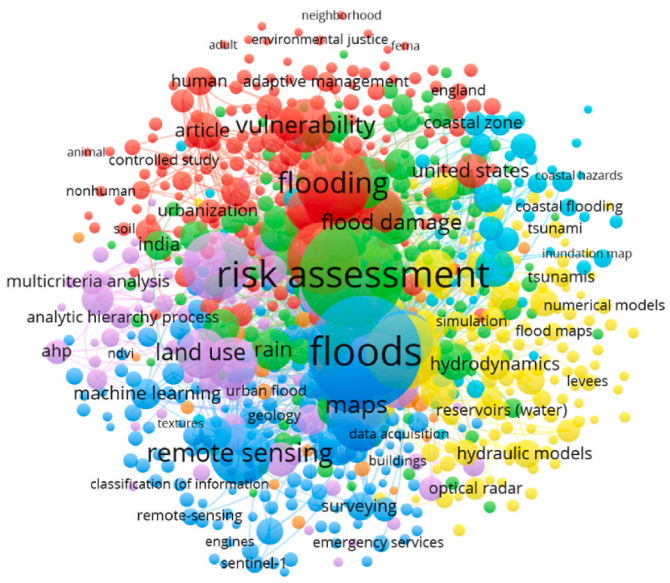

Fig. 1. Co-occurrence matrix for Flood Risk Map 1816 keywords, threshold meet 776 of 12 occurrences.

are 24°50′N - 24°75′N & 72°00′E – 72°45′E respectively (see Fig. 2). The watershed covers an approximate area of 442 km^2. The watershed exhibits a varied topography, with the western hills being higher, forming part of the Mt. Abu range. The general slope of the terrain follows a NE to SW direction, with the lowest point located near the Dhanera district. The watershed area has been further divided into 52 micro watersheds, each with different soil types, such as clay, sand, and coarse loam. The region experiences a hot semi-arid climate, with a maximum dry temperature ranging around 46 °C during summer. The area is predominantly inhabited by tribal populations, historically dependent on forests for their livelihood and now practicing subsistence agriculture. There is steep slope in upper Rel River catchment, leading to flash floods during heavy rainfall. In 2017, the region experienced the heaviest rainfall in the past century, resulting in catastrophic flooding in Dhanera and surrounding areas [33]. The absence of discharge capacity of the river, combined with heavy rainfall, led to severe flooding, causing numerous casualties and extensive property damage.

According to the Indian Meteorological Department (IMD), the state received 559.4 mm of rainfall from July 1 to 28, exceeding the average of 339.6 mm for this period by 65 %, indicating significant excess precipitation. On July 24, several districts in northern Gujarat experienced over 200 mm of rainfall within 24 h. Dhanera specifically received 231 mm in just 6 h on July 24, followed by 275 mm and 139 mm on the next consecutive days. The flooding in Dhanera was caused by the discharge from Jetpura and Rauva Dams in Rajasthan, which combined with the Rel River's waters. The rainfall was near the highest in 112 years for the region. Dhanera, with a population of 30,000, faced severe flooding, with water levels rising up to 3050 mm (10 feet), isolating the town for 48 h as all access roads were submerged. The flooding not only disrupted transportation but also led to the collapse of power and telecommunication lines, exacerbating the challenges faced by the affected community.

The risk map was meticulously prepared by integrating various hazard and vulnerability indicators to assess potential risks in the study area. Key data sources included Landsat satellite imagery, which was utilized to generate the Land Use/Land Cover (LULC) map, accessed through the Earth Explorer platform (https://earthexplorer.usgs.gov/accessed on Nov 12, 2023). Rainfall data were obtained from the CHIRPS pentad dataset, accessed via the Google Earth Engine (GEE) platform (https://chc.ucsb.edu/data/chirps accessed on Nov 15, 2023). Additionally, the Digital Elevation Model (DEM) was constructed using Shuttle Radar Topography Mission (SRTM) data, processed on the GEE platform (https://cmr.earthdata.nasa.gov/search/concepts/C1000000240-LPDAAC_ECS.html accessed on Nov 15, 2023). Each of these datasets was crucial for providing a comprehensive and accurate representation of the risk factors and environmental conditions analyzed in the research.

The risk map was prepared using various hazard and vulnerability indicators. The LULC was generated using Landsat satellite imagery (https://earthexplorer.usgs.gov/accesses on Nov 12, 2023). The rainfall data was extracted using GEE from CHIRPS pentad (https://chc.ucsb.edu/data/chirps accessed on Nov 15, 2023). The DEM was prepared in GEE platform using SRTM datasets (https://cmr.earthdata.nasa.gov/search/concepts/C1000000240-LPDAAC_ECS.html accessed on Nov 15, 2023). The various datasets were used for the analysis provided in

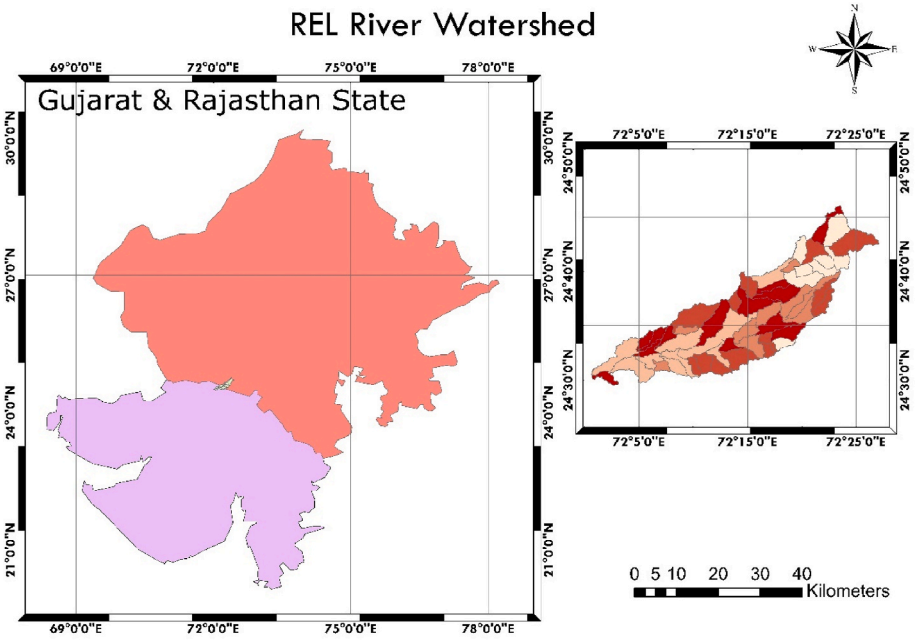

Fig. 2. The map illustrating the geographical location of the Rel River Watershed in Gujarat, India.

Table 1
Datasets used for hazard and vulnerability indicators.

Sr. No.	Dataset	Spatial Resolution	Derived Map
1	Landsat 8 Operational Land Imager (OLI)	30 m	LULC
2	Climate Hazards Group InfraRed Precipitation with Station (CHIRPS Pentad, Version 2.0 Final)	0.05°	Rainfall
3	SRTM (NASA) Digital Elevation	30 m	Elevation, Slope, Flow Accumulation
4	Google Earth Imagery	–	Distance to hospital
5	District Census Handbook	–	Population density map

Table 1.

3. Methodology

The assessment of flood risk within Rel River watershed employed a combination of five flood hazard indicators (Soil, elevation, slope, flow accumulation, and rainfall) and three flood vulnerability indicators (LULC, Distance to hospital, and population density). AHP method was implemented to assign the weightage to all eight parameters, which was used to prioritize and rank the 52 micro-watersheds of Rel River for flood risk (Fig. 3). Integration of GEE, Spectral indices for obtaining various hazard & vulnerability indicators, which were prioritized and ranked using AHP for preparing flood map is a unique methodology, thus facilitating a robust evaluation of flood risk mapping across the study area.

3.1. Flood hazard indicators

The soil datasets were procured from the NBSS & LUP and subsequently converted it into a comprehensive soil map for the study area. The transformation process involved leveraging GIS tools to visually represent the distribution and characteristics of different soil types across the designated landscape. The resulting soil map serves as a valuable flood hazard indicators for offering insights into the spatial variations of soil properties within the study area. An elevation map, a slope map, and a flow accumulation map were prepared using SRTM - DEM data by employing the Google Earth Engine (GEE). The Earth Engine platform facilitated efficient and scalable geospatial analysis. The elevation map illustrates the varying heights across the terrain, providing a comprehensive overview of the topographical features. Simultaneously, the slope map highlights the gradient variations, offering key information on the steepness of different landforms. Additionally, a flow accumulation map was generated, showcasing the accumulated water flow paths. A comprehensive rainfall map was prepared using CHRIPS pentad data processed in GEE. The Earth Engine platform facilitated efficient analysis of CHRIPS pentad data over the study area, to derive precipitation patterns resulting in rainfall map. Supplementary, the rainfall data from SWDC (State Water Data Center)

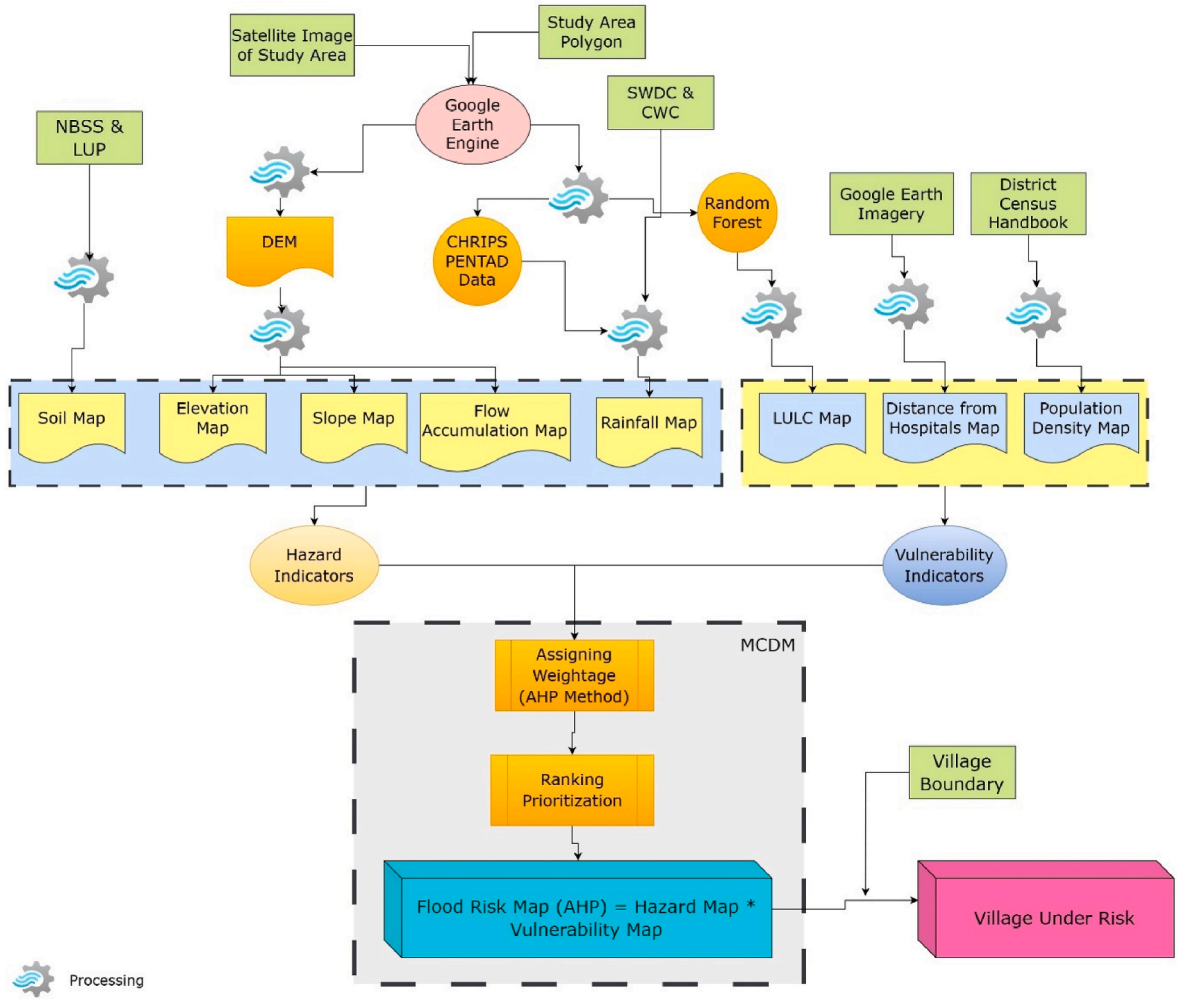

Fig. 3. Methodology signifying the usage of RS-GIS, GEE, and AHP techniques for formulating Flood Risk Map and Villages under risk.

and CWC (Central Water Commission) were incorporated to enhance the accuracy and reliability of the rainfall map. The amalgamation of these datasets offers a robust representation of the spatial distribution of rainfall map across the study area. These processed maps serve as essential flood hazard indicators for understanding and visualizing the geographical characteristics of the study area.

In order to assess the risk of flooding, soil type is crucial. Areas that have sandy soils that can absorb water quickly are less likely to flood. Flood danger exists in areas with top-notch particles that prevent water infiltration. The grained soil makes up around 85.71 % of the study area, which makes the area more vulnerable to flooding. Greater regions at risk of flooding are indicated by better values. Flow accumulation ranged from 0 to 2322 m^3 in the study area, identifying areas susceptible to severe flooding. Using GIS, maps of the spatial distribution of five significant FHI were produced, facilitating the visualization of the study area inundation regions. Understanding these variables indicated in Table 2 helps identify the places that are more exposed to flooding. Elevation and slope have an inverse relation with flood, while rainfall, soil, and flow accumulation have a direct relation with flood (Table 2).

3.2. Flood vulnerability indicators

LULC map preparation is a vital flood vulnerability indicator and it was prepared in GEE platform by processing the Landsat 8 satellite imagery. In order to assure accuracy and consistency across the images, data preparation and calibration are usually the first steps in the classification process. The initial data preparation stage is made simpler by GEE's built-in image pre-processing features, which include atmospheric correction, cloud and shadow masking, and radiometric calibration. Google Earth Engine is used for LULC classification using Machine learning algorithms i.e., Random Forest. Surface reflectance of Landsat 8 data sets has processed for cloud and temporal filtering to obtain time series of dataset for temporal analysis. GEE offers functions for implementing algorithms, and users can alter the options and parameters to suit their unique research requirements. Identified training samples that are typical of the various land cover classes are needed for the classification model's training. To create the training samples, GEE permits the inclusion of ground truth data, such as field surveys or current land cover maps. Seventy percent of these samples are utilized to train the machine learning model, allowing it to discern patterns and spectral signatures associated with various types of LC. The trained model is then applied to the entire dataset of satellite images to generate the LULC classification map. Thirty percentage of the identified classes datasets has been used to validate the results. Based on the correlation matrix and kappa coefficient the accuracy for the model is obtained for LULC classification. The second important indicator i.e., distance from the hospitals was obtained from Google Earth and processed using ArcGIS 10.3. Leveraging the detailed visual data provided by Google Earth, the vicinity was assessed and mapped, and the proximity and ease of access to hospitals in the study area. The imagery served as a valuable resource for accurately depicting the spatial distribution of healthcare facilities, enabling to analyse and visualize accessibility patterns. The third important indicator i.e., population density, the district census data was harnessed to construct a population density map using ArcGIS 10.3. The resulting population density map provides a clear depiction of the concentration of inhabitants across different areas of study, offering valuable insights for flood planning and mitigation, relief resource allocation, and demographic analysis within the specified geographic area.

Understanding these variables indicated in Table 3, helps identify the places that are more vulnerable to flood. LULC has inverse relation with flood, while population density and distance to hospital has direct relation with flood as indicated in Table 3.

Table 2
The functional relationships between the various flood hazard indicators.

Indicators	Significance	Functional Relation	References
Elevation	Level of inundation	Inverse	[42,44–52]
Slope	Runoff from the surface	Inverse	[17–19, 21–53]
Rainfall (Annual avg.)	Run-off production	Direct	[54]
Soil	Flood risk mitigation capacity is dependent on intrusion rate; a high intrusion rate reduces the likelihood of flooding.	Direct	[41]
Flow accumulation	Finding flood-prone areas: High flow buildup indicates a possible high flood hazard	Direct	[41]

3.3. AHP

The AHP proves to be a valuable methodology when applied to flood risk mapping, offering a systematic and structured approach to decision-making in the intricate field of FRA. AHP entails the systematic breakdown of the flood risk mapping process into a hierarchical structure that commonly includes a defined goal, criteria, and alternative options. Within the context of flood risk, criteria encompass elements such as topography, land use, precipitation patterns, infrastructure, and historical flood data. The utilization of AHP in flood risk mapping enables decision-makers to methodically assess and prioritize these criteria, resulting in more informed and efficient strategies for mitigating and managing the associated risks of flooding.

The preparation of FRM has been computed through the stacking of flood indices, specifically the FHI and FVI. This was achieved by employing a weighted sum overlay method, utilizing raster layers of all eight identified flood causative hazards and vulnerability indicators. The relative significance of each indicator was determined by assigning ranks based on expert opinions and information from published literature. To establish the relative weights for each raster layer, a MCDM approach using the AHP technique was implemented. This involved the spatial analyst tool in ArcGIS software, allowing for the generation of FHI and FVI maps based on specific expressions outlined in equations (1) and (2). These indices serve as valuable tools for spatially assessing and understanding the potential risks associated with hazard and vulnerability.

$$FHI = (W_{ELV} \times ELV) + (W_{SLP} \times SLP) + (W_{RF} \times RF) + (W_{SL} \times SL) + (W_{FA} \times FA) \quad (1)$$

Where W_{ELV}, W_{SLP}, W_{RF}, W_{SL}, and W_{FA} are the corresponding normalized weights for each indicator. ELV, SLP, RF, FA, and SL refer to elevation, slope, rainfall, soil, and flow accumulation.

$$FVI = (W_{PD} \times PD) + (W_{LULC} \times LULC) + (W_{DH} \times DH) \quad (2)$$

where W_{PD}, W_{LULC}, and W_{DH} are the corresponding normalized weights of each indicator. PD, LULC, and DH stand for the population density, land use land cover, and distance to health centres (Accessibility to

Table 3
The relationships between the various flood vulnerability indicators.

Indicator	Significance	Functional Relation	Reference
Population density	Flooding's effects on assets related to the economy and population	Direct	[12]
Land use land cover	Surface intrusion and runoff, as well as financial resources in case of flooding	Inverse	[17–19, 21–51]
Distance to hospital	Other crucial factors to take into account include sanitation, hygiene, and the avoidance of waterborne infections.	Direct	[42]

hospitals).

3.4. Flood risk map

The synthesis of these two indicators i.e., hazard and vulnerability map, yields a flood risk map (Equation (3)). This comprehensive map integrates the likelihood of flood hazards with the potential consequences and vulnerabilities of the study areas. By combining these elements, decision-makers gain a nuanced understanding of where and to what extent flooding may pose risks to communities. This integrated approach is instrumental in formulating effective flood management strategies, emergency response plans, and land-use policies to mitigate the overall impact of flooding on both people and infrastructure. In essence, the flood risk map provides a holistic perspective, essential for fostering resilience and sustainable development in flood-prone regions.

$$Flood\ Risk\ Map = Flood\ Hazard * Flood\ Vulnerability \quad (3)$$

4. Results & discussions

The current investigation utilized an integrated approach, seamlessly combining five flood hazard indicators and three flood vulnerability indicators refined with Google Earth Engine (GEE) datasets. This integration, along with the AHP-MCDM approach, GIS, and remote sensing techniques, facilitated a detailed ranking of 52 micro-watersheds for flood risk. The outcome was the identification and mapping of flood risk zones, categorized as very low, low, moderate, high, and very high, within the Rel River watershed and the villages at risk in Gujarat state. The Flood Vulnerability Index (FVI) and Flood Hazard Index (FHI) indicators drew insights from diverse data sources, contributing to a comprehensive understanding of flood dynamics. The resulting maps of these flood risk indicators were meticulously developed and systematically examined, providing insights into the nuanced aspects of flood risk severity across the study area.

4.1. Elevation map

The SRTM dataset, featuring a spatial resolution of 30 m (Fig. 4), was employed to generate an elevation map and define the boundaries of watersheds. The elevation is drastically changing in watershed from 787 m to average of 10–22 m above MSL in study area. Utilizing the ArcHydro tool 10.3, the process was conducted to delineate micro-watershed & stream boundaries within the region. The topographical elevation significantly impacts water flow and the likelihood of flooding during flood events. Areas with higher elevations typically have a lower flood risk, whereas lower-lying regions are more prone to inundation. Elevation maps play a crucial role in simulating water flow scenarios and modeling potential floods. Integrating elevation data with other factors, including rainfall patterns, soil properties, and land use, allows for the creation of flood risk maps. These maps offer a comprehensive representation of areas with diverse levels of risk, facilitating the development of well-informed mitigation strategies and emergency response plans.

4.2. Soil map

Soil layers were extracted using data provided by the NBSS & LUP. A soil map at a scale of 1:50,000 was then created, as depicted in Fig. 5. Various soil types exhibit distinct volumes for holding rainwater. In the study area, the primary focus for flood risk mapping was on the prevalent soil textures. The study area comprises five distinct soil texture types, namely coarse loamy, hill soil, sandy soil, sandy to clay loam & sandy to sandy loam. During rainy season the soil infiltration capacity plays a vital part in the absorption of water. A high infiltration capacity indicates a low flood risk, and consequently, areas with a very low category signify those in the high flood hazard zone.

4.3. Slope map

The slope map was classified into 5 classes, as illustrated in (Table 4). Utilizing the ArcHydro tool 10.3, the process was conducted to delineate micro-watershed boundaries & streams within the designated region. The slope map illustrated in Fig. 6 serves as a vital tool in the development of flood risk maps, playing a crucial role in understanding the terrain's impact on water movement during flood events. The degree of slope directly influences the speed and direction of water flow, affecting the severity of potential flooding. Steeper slopes tend to accelerate water runoff, potentially leading to higher flood risks in downstream areas. The slope varies from 0 to 787 m for the study area with colour variation from light purple to dark brown (Fig. 6). In contrast, gentler slopes allow

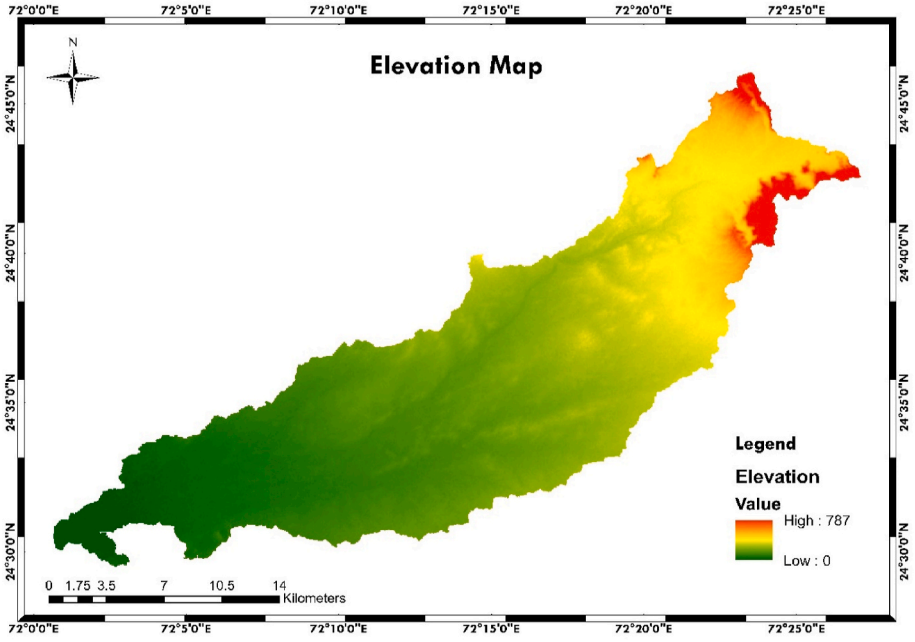

Fig. 4. Elevation Map of the study area.

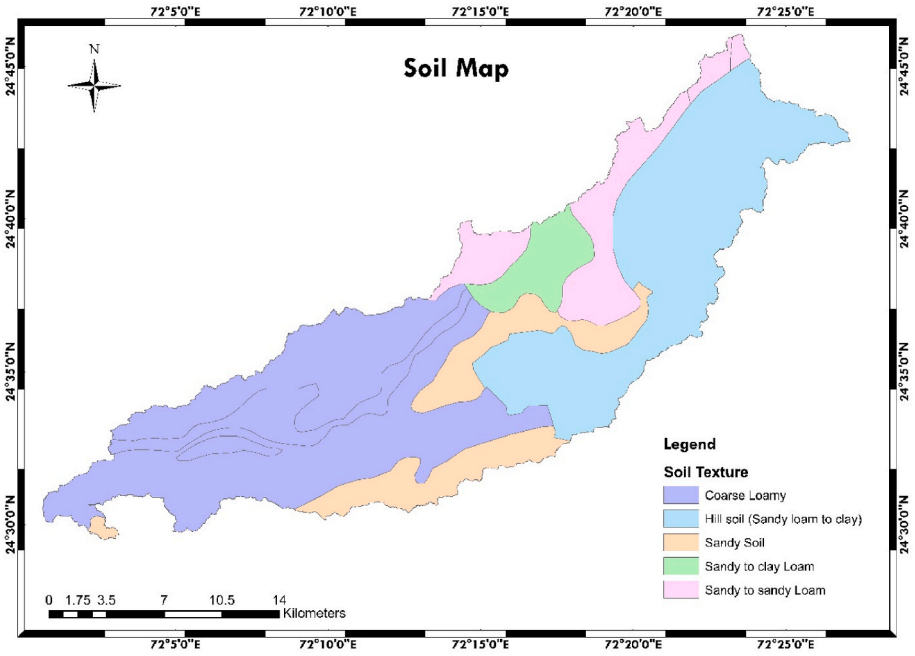

Fig. 5. Soil Map of the study area.

Table 4
Weightage of Indicators for determining the flood events.

Indicators	Old parameter	New Parameter	Weight
Elevation	Low = 0–120 m	1	0.15
	120–250 m	2	
	250–390 m	3	
	390–580 m	4	
	High = 580–787 m	5	
Soil	Coarse Loamy	1	0.0526
	Hill Soil	2	
	Sandy Soil	3	
	Sandy to Clay Loam	4	
	Sandy to Sandy Loam	5	
Slope	High = Peak (787 m)	5	0.16
	Steep Slope	4	
	Upper Slope	3	
	Lower Slope	2	
	Low = Valley (0 m)	1	
Flow Accumulation	Very Low = 1–465 m^3	1	0.175
	465–929 m^3	2	
	929–1394 m^3	3	
	1394–1858 m^3	4	
	Very High = 1858–2322 m^3	5	
Precipitation	25–28 cm/day	1	0.121
	28–31 cm/day	2	
	31–34 cm/day	3	
	34–37 cm/day	4	
	37–40 cm/day	5	
LULC	Urban	1	0.17
	Barren	2	
	Water	3	
	Agriculture	4	
	Scrubland	5	
Distance from Hospital	Easily Reachable	1	0.0934
	Near	2	
	Far	3	
	Very Far	4	
	Difficulty to Reach	5	
Population (per square km)	0–100	1	0.078
	100–200	2	
	200–500	3	
	500–750	4	
	750–1000	5	

for more gradual water movement, reducing the risk of rapid inundation. By incorporating slope data into flood risk mapping along with other factors such as elevation, land use, and soil characteristics, a comprehensive assessment of flood vulnerability can be achieved. The result is a detailed flood risk map that considers the complex interplay of terrain features.

4.4. Flow accumulation map

The flow accumulation map illustrated in Fig. 7 serves as a pivotal tool in the creation of flood risk maps, providing essential insights into the accumulation and concentration of water flow across a landscape. It is a key component in understanding the potential pathways and areas prone to increased water volume during flood events. By considering indices such as slope and terrain, the flow accumulation map contributes to a comprehensive flood risk assessment. The flow accumulation categorises in five categories i.e., very low (1–465 m^3), low (465–929 m^3), moderate (929–1394 m^3), high (1394–1858 m^3) and very high (1858–2322 m^3) on the basis of the volume of water flow. This map aids in visualizing where water converges, potentially leading to heightened flood risks. When integrated with other crucial factors like elevation, rainfall patterns, soil characteristics, and land use, the flow accumulation map contributes to a holistic flood risk map. The resulting map is a detailed and accurate representation of areas with varying degrees of susceptibility to flooding.

4.5. Rainfall map

The rainfall map (see Fig. 8), a hazard indicator, plays a key role as a tool in the development of flood risk maps, providing crucial information about precipitation patterns that directly influence the likelihood of flooding. By analyzing rainfall data across a specific area, flood risk assessments can be enhanced by identifying regions prone to heavy rainfall and potential inundation. There was occurrence of heavy rainfall during July 2017 in range of 25 cm/day to 40 cm/day. The runoff from this heavy rainfall was very high and resulted to severe flash flood. When rainfall integrated with other key factors such as topography, soil type, land use, and the existing drainage network Rainfall maps contribute to a comprehensive flood risk analysis. Understanding the

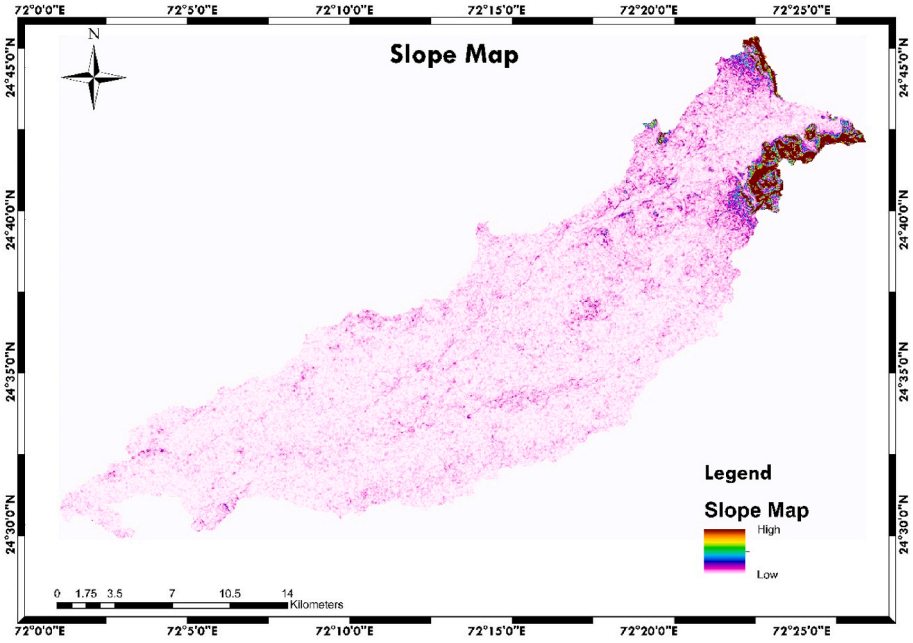

Fig. 6. Slope Map of the study area.

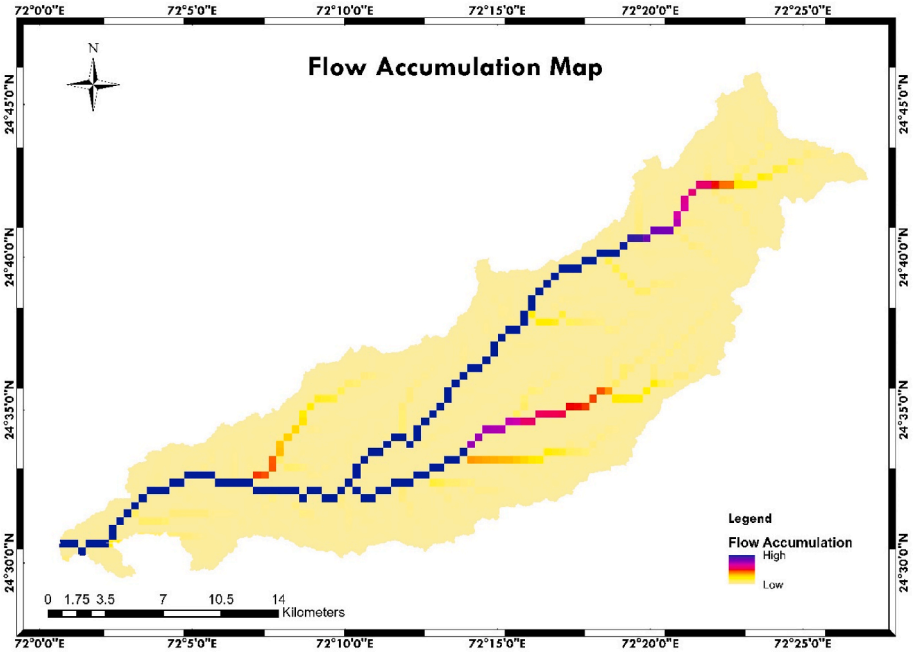

Fig. 7. Flow Accumulation Map of the study area.

spatial distribution and intensity of rainfall allows for more accurate predictions of potential flood scenarios.

4.6. LULC map

LULC map is one of the vulnerability indicators, and describes five categories agriculture land, urban area, scrubland, water, and barren land, as illustrated in (Table 4). LULC mapping using GEE and the RF algorithm was implemented in the present study. Multiple decision trees are used in RF, an ensemble learning technique, to increase classification accuracy and manage intricate interactions between features and classes. For LULC mapping, the RF algorithm performed exceptionally well. It classified the land cover classes with a kappa value of 0.94 and an overall accuracy of 95 %, suggesting an efficient and highly precise classification as indicated in Fig. 9. LULC maps serve as indispensable tools in the formulation of flood risk maps, providing critical insights into the utilization and characteristics of the land that significantly influence flood dynamics. These maps categorize and depict the different types of land use, such as urban areas, agricultural fields, and natural vegetation, along with land cover features like forests, water bodies, and impervious surfaces. LULC information is essential in understanding how human activities and natural features interact to impact surface runoff and water absorption. When integrated with other factors such as topography, rainfall patterns, soil properties, and the existing drainage network, LULC maps contribute to a comprehensive flood risk assessment. The result is a detailed LULC map that considers the complex

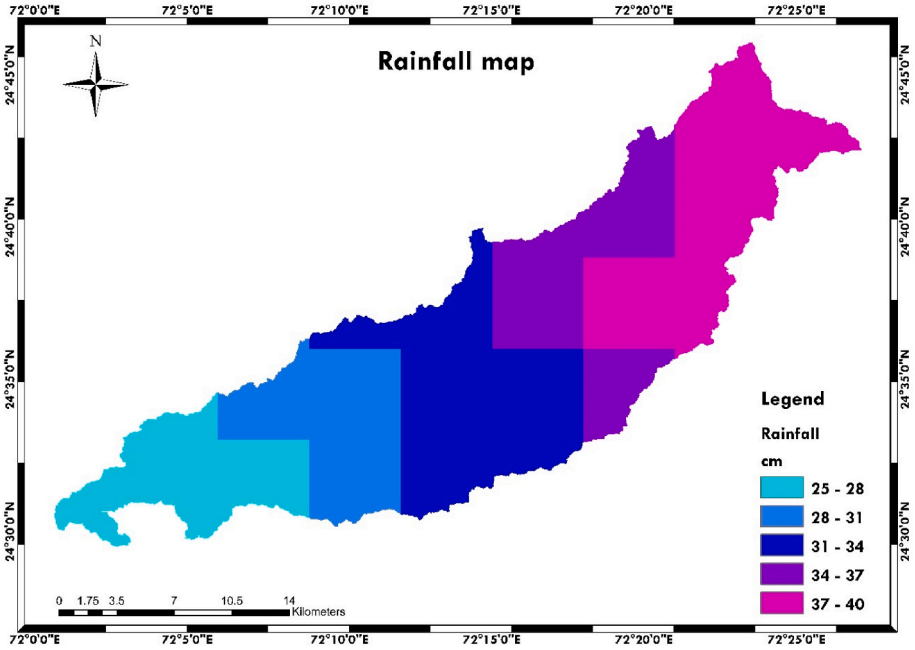

Fig. 8. Rainfall Map of the study area.

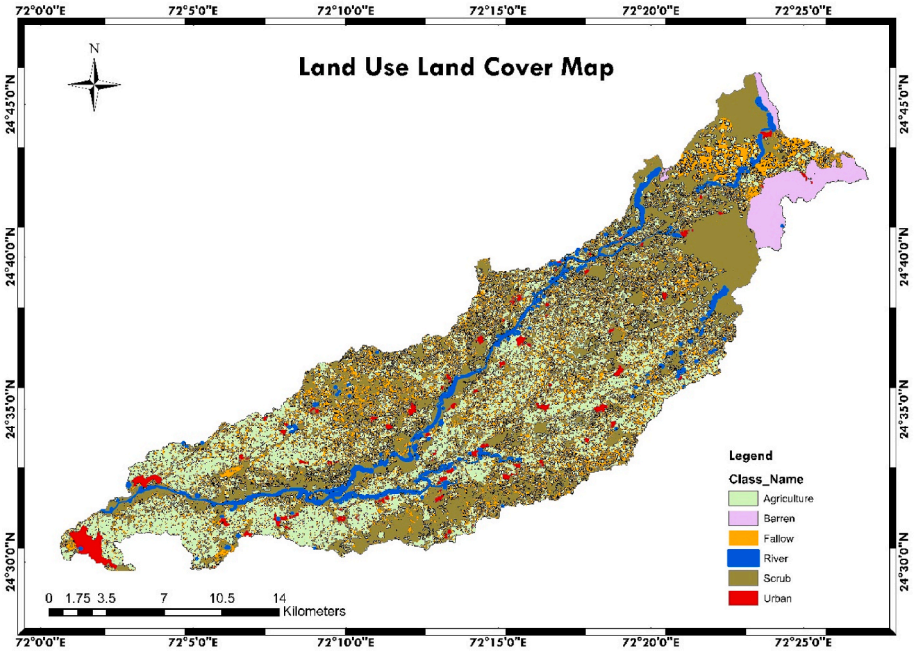

Fig. 9. Land Use Land Cover Map of the study area.

relationships between land use, surface characteristics, and flooding, providing valuable information for the development of effective flood mitigation and response strategies.

4.7. Distance to hospitals

The distance to hospital map is a vulnerability factor, as demonstrated in Fig. 10, a crucial tool in the development of flood risk maps, incorporating considerations beyond traditional hydrological factors. This map assesses the proximity of healthcare facilities to various locations within a region vulnerable to flooding. It plays a vital role in emergency preparedness and response planning, as accessibility to hospitals is paramount during flood events when swift medical assistance is often required. Integrating the distance to hospital map with other factors such as topography, rainfall patterns, land use, and demographic data provides a holistic understanding of flood vulnerability. The distance to hospital was extracted and analyse with the help of google earth. Further, the location was processed to generate the vicinity of the hospital by implementing the interpolation technique used in the ArcGIS 10.3. This vulnerability indicator helps in a comprehensive flood risk mapping that not only highlights areas prone to inundation but also identifies regions with limited access to healthcare facilities during emergencies. Accessibility to hospital map describes five categories easily reachable, nearby, far, very far, and difficult to reach as illustrated

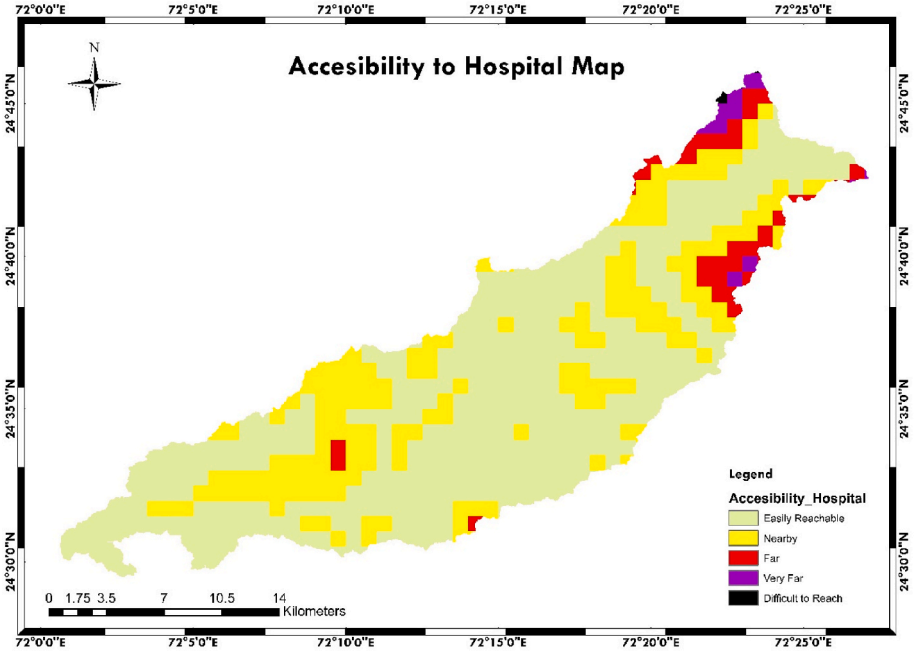

Fig. 10. Accessibility to hospitals/distance to hospital Map of the study area.

in (Table 4). This information is instrumental in formulating targeted evacuation plans, allocating resources effectively, and enhancing overall disaster resilience within the affected communities.

4.8. Population density

The population density is also an important vulnerability indicator, illustrated in Fig. 11 serves as a valued tool in the comprehensive development of FRM, incorporating a socio-demographic dimension to the analysis. The population density of ranges in different category (population count per square km) i.e., 0–100; 101–200; 201–500; 501–750; and 751–1000. The weightage of each category was assigned with the help of the AHP-MCDM technique to prepare the flood vulnerability map. This map provides crucial insights into the concentration of inhabitants across a given area, allowing for an understanding of potential human vulnerability during flooding events. When integrated with other factors such as topography, rainfall patterns, land use, and infrastructure, the population density map contributes to a holistic flood risk assessment. It helps identify areas with high population density that may be more susceptible to the impacts of flooding, aiding in the formulation of targeted evacuation plans, resource allocation, and emergency response strategies.

4.9. Flood hazard map

The flood hazard map serves as a fundamental tool in the

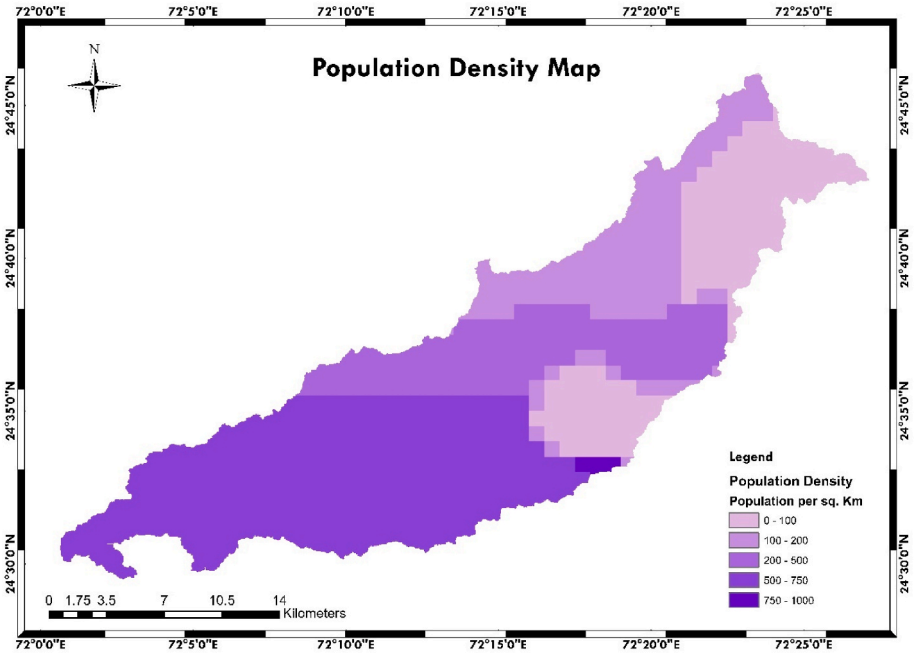

Fig. 11. Population density Map of the study area.

development of flood risk maps, offering a specialized focus on identifying areas susceptible to potential flooding based on various factors. This map incorporates an analysis of flood-prone zones, considering five factors elevation map, slope map, rainfall patterns, soil characteristics, and flow accumulation map. The flood hazard indicator was calculated by integrating the all factors and prepare the flood hazard map (Fig. 12). The map provides a comprehensive understanding of the physical conditions that contribute to flooding. The result is a detailed depiction of areas at varying levels of flood hazard, allowing for a nuanced assessment of potential risks into five categories from very high to very low. This map becomes an integral part of the overall flood risk assessment, enabling the formulation of effective mitigation strategies, land-use planning, and emergency response plans to protect communities and infrastructure from the impacts of flooding.

4.10. Flood vulnerability map

The flood vulnerability map is a critical tool in the construction of flood risk maps, offering a nuanced perspective on areas vulnerable to the impacts of flooding based on a range of three factors. These factors i.e., population density, accessibility to hospitals, & LULC factors were considered to estimate the FVI and processed for the preparation of flood vulnerability map (Fig. 13). The flood vulnerability map provides a comprehensive understanding of the potential human and societal risks associated with flooding. The result is a detailed depiction of regions with varying degrees of vulnerability, facilitating a detailed flood risk assessment. By integrating these diverse factors with information on topography, rainfall patterns, and land use vulnerability map becomes instrumental in the development flood risk map.

4.11. Flood risk map

"Risk" means there could be harsh weather or long rains which could lead to floods. To evaluate flood risk within the Rel River watershed, a comprehensive approach was adopted, utilizing a combination of five flood hazard indicators (Soil, elevation, slope, flow accumulation, and rainfall) and three flood vulnerability indicators (Land Use and Land Cover, Distance to hospital, and population density). The AHP-MCDM technique was applied to assign weights to all eight parameters, providing a systematic means to prioritize and rank the 52 micro-watersheds of the Rel River based on their flood risk. This methodological integration aims to capture the multifaceted nature of flood risk, considering both physical factors contributing to hazards and socio-environmental vulnerabilities and processed for flood risk map (Fig. 14). The weighted combination of these indicators facilitates a nuanced understanding of flood risk distribution across the watershed, enabling informed decision-making and targeted interventions for effective flood risk management.

The weight assigned to each criterion is represented as a percentage of the overall weight of all criteria and is established through a pairwise comparison process (Table 4). This process entails comparing each criterion with every other criterion to ascertain their relative importance. The comparison is conducted on a scale ranging from 1 to 5, where 1 signifies very low importance, 3 indicates moderate importance, and 5 indicates very high importance.

Fig. 14 illustrate flood risk map employing AHP multi criteria decision method, describing color-coded topographic map of 52 micro-watersheds flood risk intensity. The intensities are labeled as "Very High", "High", "Medium", "Low", and "Very Low", each likely associated with a color from light brownish red to dark brownish red color. Each micro watershed risk and total area in various risk categories from very high to very low is described in Table 5.

4.12. Validation

The flood risk map, developed through the integration of flood hazard and vulnerability maps using the Multi-Criteria Decision Analysis (MCDA) method, underwent a thorough validation process against a satellite-based historical inundation map. The validation results indicate that approximately 48 % of the total inundation area falls within high and very high-risk zones, while the remaining 52 % is distributed across very low to moderate-risk zones.

An examination of the spatial distribution of land use types concerning the index-based hazard zones and the satellite-derived inundation map reveals that urban and agricultural areas are particularly vulnerable to floods, followed by scrubland. The average contribution of each land use type (excluding water and barren land) to the moderate to very high hazard zones closely align ($R^2 = 0.98$) with the corresponding

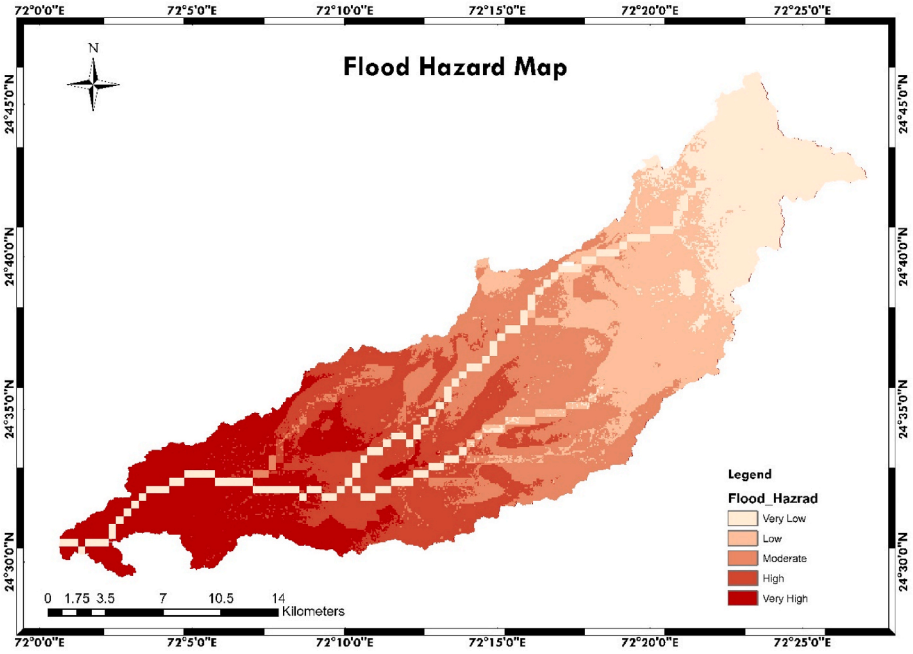

Fig. 12. Flood hazard intensity.

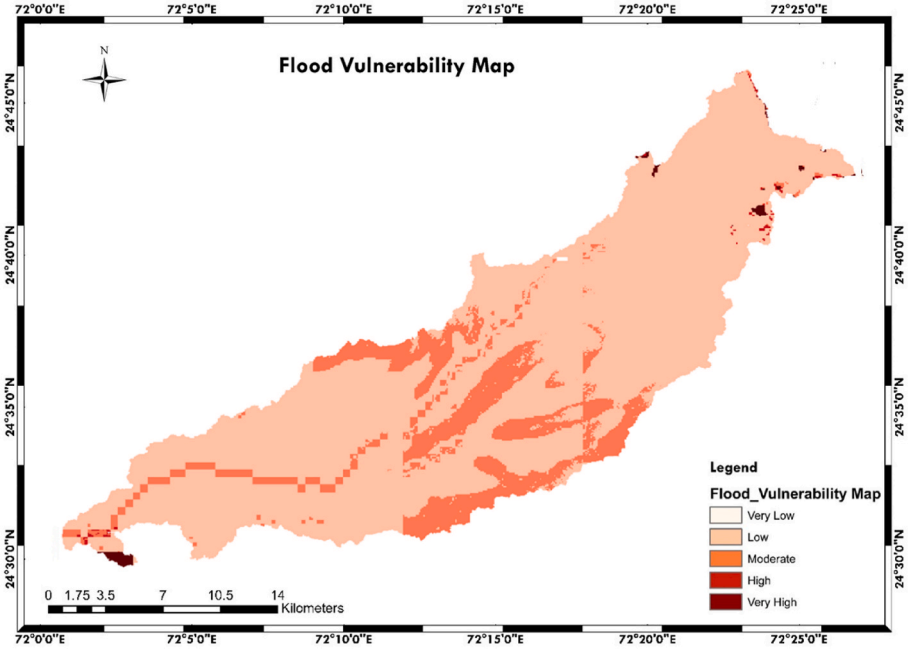

Fig. 13. Flood vulnerability map.

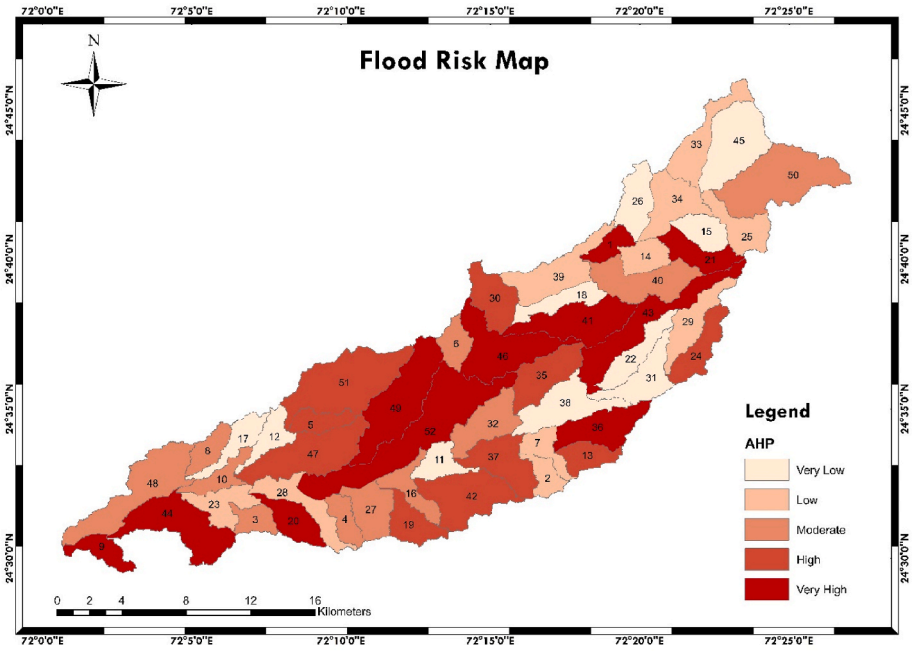

Fig. 14. Flood risk mapping delineates 52 micro-watersheds, ranging from very high to very low risk.

Table 5
FRM delineates 52 micro-watersheds, ranging from very high to very low risk along with the area.

Risk	Micro-watersheds no.	Area (km^2)
Very Low	11, 12, 15, 17, 18, 22, 26, 31, 38, 45	69.36
Low	2, 7, 14, 23, 25, 28, 29, 33, 34, 39	68.07
Moderate	3, 4, 6, 8, 10, 13, 16, 27, 32, 40, 48, 50	90.98
High	5, 19, 24, 30, 35, 37, 42, 47, 51	88.62
Very High	1, 9, 20, 21, 36, 41, 43, 44, 46, 49, 52	124.53

contribution to the satellite-derived inundation map. This close correlation underscores the realism of the estimated index-based flood hazard zones, demonstrating a consistent alignment with the observed inundation events. Overall, the validation analysis reinforces the reliability of the developed flood risk map and its capability to accurately depict flood-prone areas based on historical inundation data.

4.13. Village at risk

The Flood risk map for administrative boundaries of village/taluka in Rel River watershed, Gujarat and Rajasthan state (Fig. 15). The map illustrating villages under flood risk serves as a crucial tool in disaster preparedness, mitigation, and response efforts. This map provides a

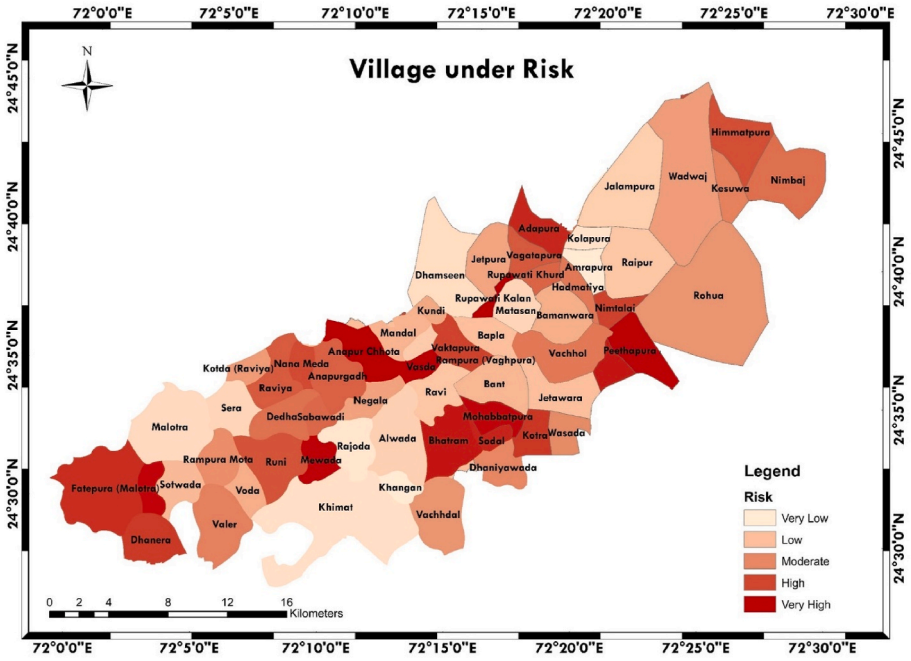

Fig. 15. Flood risk map for administrative boundaries of village/Taluka in Rel River watershed, Gujarat and Rajasthan state.

clear visual representation of areas susceptible to flooding, enabling authorities and communities to identify high-risk zones. This information is invaluable for developing targeted evacuation plans, allocating resources effectively, and implementing proactive measures to enhance community resilience. Additionally, it aids in communicating risk levels to the public, fostering awareness, and guiding land-use planning decisions. The utility of a flood risk map extends beyond immediate response, contributing to long-term strategies for sustainable development and disaster risk reduction in vulnerable areas.

Based on the Census 2011 data, the demographic distribution in the Rel River watershed reveals that the area covered in Gujarat state is home to 90,485 people, with 46,944 male and 43,541 female residents whereas, 32,890 individuals reside in the area covered in Rajasthan state, comprising 17,033 males and 15,857 females. The census data also sheds light on literacy levels, a crucial factor in flood warning system effectiveness. In Gujarat, the male population exhibits a literacy rate of 23,541, while the female population has a literacy rate of 9,303, resulting in a total of 32,844 literate individuals. Similarly, in Rajasthan, the male population demonstrates a literacy rate of 8,457, and the female population has a literacy rate of 3,544, accounting for a total of 12,001 literate individuals. Recognizing these demographic and literacy statistics is vital for enhancing flood mitigation measures and developing effective flood warning systems, particularly considering the importance of literacy in ensuring the dissemination and comprehension of timely alerts and information.

5. Recommendations

- ➢ Appropriate institutional arrangements should be established between Gujarat and Rajasthan to enhance readiness for potential flooding in the Rel River, given that both states share the catchment areas of these river systems.
- ➢ Creating user-friendly Smart Apps for the state of Gujarat is crucial. Technology played a significant role in facilitating evacuation, providing alerts to people in high-risk and remote areas.
- ➢ Implementing sustainable management practices for sand mining is essential for the Rel River. Currently, there is a substantial accumulation of sand in the river. Extracting this sand at the present stage for construction purposes could significantly decrease the sediment load.
- ➢ The location currently lacks rain gauges which are essential, and there is a critical need to install automatic gauges to alleviate data deficiencies in hydrologic, hydraulic, or hydrodynamic modelling. Conducting a thorough study is essential to identify suitable locations for the installation of these gauges.
- ➢ The entire methodology is designed in the absence of sufficient data. In the future, it is imperative to conduct on-site execution, testing, and surveys to minimize uncertainties in the parameter weights within the AHP method. Currently, the weights are determined primarily based on expert opinions.
- ➢ Training walls must be consistently designed as Reinforced Cement Concrete (RCC) structures instead of the previously employed coarse rubble masonry. The latter may prove insufficient in withstanding severe floods, as demonstrated by the experience with the Dantiwada dam during the floods of 2017.
- ➢ The preparation of the Flood Risk Map does not currently take into account inundation map, flow velocity, water depth, and estimated arrival time in flood plain regions. In the future, it is recommended to explore high-resolution DEMs, hydrodynamic modelling, and advanced satellite approach in this region. This exploration will aid in quantifying the level of flood vulnerability and reducing modelling uncertainties, ultimately enhancing the decision-making system for flood risk management.

6. Conclusion

Floods pose a constant and global threat, with their impact exacerbated by socioeconomic developments, urbanization, ineffective drainage systems, and insufficient river control measures. The state of Gujarat, particularly the region around the Rel river in Dhanera, is no exception to this menace. The monsoon season brings with it a heightened risk of flooding, placing immense strain on the area's infrastructure and inhabitants. A detailed study was undertaken, employing geospatial techniques to divide the study region into 52 micro-watersheds. These micro-watersheds serve as focal points for analysing flood hazards, vulnerabilities, and risks. The study utilized morphometric analysis to examine the morphology of the area, providing valuable insights into

the topographical features that contribute to flooding. Further, the AHP-MCDM methodology was employed to assign weights, priority ranks, and risk categories to each micro-watershed, facilitating a nuanced understanding of the flood risk landscape. The mapping of flood hazard zones was delineated, with vulnerability assessments ranging from very low to very high. A holistic approach was adopted, integrating multiple criteria to determine the risk factors associated with floods. The AHP-MCDM technique played a pivotal role in estimating the normalized weights of various factors, including hazard indicators (such as soil type, elevation, slope, flow accumulation, and rainfall) and vulnerability indicators (LULC, distance from hospitals, and population density maps). Each factor was derived from Google Earth Engine (GEE), emphasizing the integration of RS and geospatial technologies in FRA. The culmination of these efforts resulted in a comprehensive flood risk map, providing a detailed analysis of vulnerability and hazard indicators across the study area. Twenty micro-watersheds were identified as highly susceptible to high to very high risks, covering an area of 213.15 km^2. In contrast, 32 micro-watersheds fell within the very low to moderate risk category, spanning an area of 228.41 km^2. This spatial differentiation is crucial for prioritizing mitigation and preparedness efforts, and directing resources where they are most needed. The uniqueness of this methodology lies in the integration of Google Earth Engine and Random Forest to obtain the vulnerability indicator i.e., LULC. The prioritization and ranking of these indicators through the AHP process contribute to the development of a robust flood map. The integrated approach enhances our understanding of flood risk dynamics, enabling more effective decision-making and resource allocation in the face of this pervasive threat. In conclusion, the study underscores the importance of a multidimensional and technology-driven approach to flood risk assessment. By leveraging geospatial techniques, morphometric analysis, and advanced decision-making methodologies, the research provides a valuable blueprint for other regions grappling with similar challenges. The integration of GEE, spectral indices, and AHP-MCDM techniques not only advances the field of flood risk mapping but also empowers communities and authorities to proactively manage and mitigate the impact of floods in vulnerable regions.

Ethics approval and consent to participate

The authors followed the ethical guidelines and no ethical approval was required and all the authors agreed to participate.

Consent for publication

All authors are agreeing to publish the content.

Availability of data and material

Data and Material will be made available on reasonable request.

Funding

Funding information is not applicable/No funding was received.

CRediT authorship contribution statement

Keval H. Jodhani: Writing – review & editing, Writing – original draft, Validation, Software, Methodology, Investigation, Data curation. **Dhruvesh Patel:** Visualization, Supervision, Methodology, Investigation, Formal analysis, Conceptualization. **N. Madhavan:** Supervision, Conceptualization. **Nitesh Gupta:** Writing – review & editing, Writing – original draft, Software, Methodology. **Sudhir Kumar Singh:** Writing – review & editing, Visualization, Supervision, Methodology, Conceptualization. **Upaka Rathnayake:** Supervision.

Declaration of competing interest

On behalf of all authors, the corresponding author states that there is no conflict of interest.

Data availability

Data will be made available on request.

Acknowledgements

The authors acknowledge the support of Pandit Deendayal Energy University, India and Nirma University, India.

References

[1] S. Gond, N. Gupta, J. Patel, P.K.S. Dikshit, Spatiotemporal evaluation of drought characteristics based on standard drought indices at various timescales over Uttar Pradesh, India, Environ. Monit. Assess. 195 (2023) 439, https://doi.org/10.1007/s10661-023-10988-2.
[2] K.H. Jodhani, K.H. Jodhani, D. Patel, N. Madhavan, Land Use land cover classification for REL river using machine learning techniques, in: 2023 International Conference on IoT, Communication and Automation Technology (ICICAT), IEEE, 2023, pp. 1–3, https://doi.org/10.1109/ICICAT57735.2023.10263663.
[3] S. Gond, N. Gupta, P.K.S. Dikshit, J. Patel, Assessment of drought variability using SPEI under observed and projected climate scenarios over Uttar Pradesh, India, Phys. Chem. Earth, Parts A/B/C 131 (2023) 103440, https://doi.org/10.1016/j.pce.2023.103440.
[4] N. Gupta, S. Gond, S.K. Gupta, Spatiotemporal trend characteristics of rainfall and drought jeopardy over Bundelkhand Region, India, Arabian J. Geosci. 15 (2022) 1155, https://doi.org/10.1007/s12517-022-10389-8.
[5] N. Gupta, A. Banerjee, S.K. Gupta, Spatio-temporal trend analysis of climatic variables over Jharkhand, India, Earth Systems and Environment 5 (2021) 71–86, https://doi.org/10.1007/s41748-021-00204-x.
[6] M. Tanoue, Y. Hirabayashi, H. Ikeuchi, Global-scale river flood vulnerability in the last 50 years, Sci. Rep. 6 (2016) 36021, https://doi.org/10.1038/srep36021.
[7] S. Bhatt, S.A. Ahmed, Morphometric analysis to determine floods in the Upper Krishna basin using Cartosat DEM, Geocarto Int. 29 (2014) 878–894, https://doi.org/10.1080/10106049.2013.868042.
[8] A. Javed, M.Y. Khanday, S. Rais, Watershed prioritization using morphometric and land use/land cover parameters: a remote sensing and GIS based approach, J. Geol. Soc. India 78 (2011) 63–75, https://doi.org/10.1007/s12594-011-0068-6.
[9] N.H. Syed, A.A. Rehman, D. Hussain, S. Ishaq, A.A. Khan, Morphometric analysis to prioritize sub-watershed for flood risk assessment in central karakoram national Park using GIS/RS approach, ISPRS Annals of the Photogrammetry, Remote Sensing and Spatial Information Sciences IV-4/W4 (2017) 367–371, https://doi.org/10.5194/isprs-annals-IV-4-W4-367-2017.
[10] N. Memon, D.P. Patel, N. Bhatt, S.B. Patel, Integrated framework for flood relief package (FRP) allocation in semiarid region: a case of Rel River flood, Gujarat, India, Nat. Hazards 100 (2020) 279–311, https://doi.org/10.1007/s11069-019-03812-z.
[11] I.M. Chathuranika, M.B. Gunathilake, H. Md Azamathulla, U. Rathnayake, Evaluation of future streamflow in the upper part of the Nilwala River Basin (Sri Lanka) under climate change, Hydrology 9 (2022) 48, https://doi.org/10.3390/hydrology9030048.
[12] A.I. Pathan, P. Girish Agnihotri, S. Said, D. Patel, AHP and TOPSIS based flood risk assessment- a case study of the Navsari City, Gujarat, India, Environ. Monit. Assess. 194 (2022) 509, https://doi.org/10.1007/s10661-022-10111-x.
[13] S. Verma, M.K. Verma, A.D. Prasad, D. Mehta, H.M. Azamathulla, N. Muttil, U. Rathnayake, Simulating the hydrological processes under multiple land use/land cover and climate change scenarios in the mahanadi reservoir complex, Chhattisgarh, India, Water 15 (2023) 3068, https://doi.org/10.3390/w15173068.
[14] K.H. Jodhani, D. Patel, N. Madhavan, A review on analysis of flood modelling using different numerical models, Mater. Today: Proc. 80 (2023) 3867–3876, https://doi.org/10.1016/j.matpr.2021.07.405.
[15] S. Hu, X. Cheng, D. Zhou, H. Zhang, GIS-based flood risk assessment in suburban areas: a case study of the Fangshan District, Beijing, Nat. Hazards 87 (2017) 1525–1543, https://doi.org/10.1007/s11069-017-2828-0.
[16] V.M. Chowdary, D. Ramakrishnan, Y.K. Srivastava, V. Chandran, A. Jeyaram, Integrated water resource development plan for sustainable management of Mayurakshi watershed, India using remote sensing and GIS, Water Resour. Manag. 23 (2009) 1581–1602, https://doi.org/10.1007/s11269-008-9342-9.
[17] D.S. Fernández, M.A. Lutz, Urban flood hazard zoning in Tucumán Province, Argentina, using GIS and multicriteria decision analysis, Eng. Geol. 111 (2010) 90–98, https://doi.org/10.1016/j.enggeo.2009.12.006.
[18] K. Jodhani, P. Bansal, P. Jain, Shoreline Change and Rate Analysis of Gulf of Khambhat Using Satellite Images, 2021, pp. 151–170, https://doi.org/10.1007/978-981-16-1303-6_12.
[19] K.H. Jodhani, D. Patel, N. Madhavan, U. Soni, H. Patel, S.K. Singh, Channel planform dynamics using earth observations across Rel river, western India: a

synergetic approach, Spatial Information Research (2024), https://doi.org/10.1007/s41324-024-00573-1.
[20] U. Vyas, D. Patel, V. Vakharia, K.H. Jodhani, Integrating GEE and IWQI for Sustainable Irrigation: A Geospatial Water Quality Assessment, in: Groundwater for Sustainable Development, Elsevier BV, 2024, p. 101332. https://doi.org/10.1016/j.gsd.2024.101332.
[21] S. Bajabaa, M. Masoud, N. Al-Amri, Flash flood hazard mapping based on quantitative hydrology, geomorphology and GIS techniques (case study of Wadi Al Lith, Saudi Arabia), Arabian J. Geosci. 7 (2014) 2469–2481, https://doi.org/10.1007/s12517-013-0941-2.
[22] F. Guzzetti, G. Tonelli, Information system on hydrological and geomorphological catastrophes in Italy (SICI): a tool for managing landslide and flood hazards, Nat. Hazards Earth Syst. Sci. 4 (2004) 213–232, https://doi.org/10.5194/nhess-4-213-2004.
[23] N. Merzi, M.T. Aktas, Geographic information systems (GIS) for the determination of inundation maps of lake Mogan, Turkey, Water Int. 25 (2000) 474–480, https://doi.org/10.1080/02508060008686856.
[24] S. Verma, M.K. Verma, A.D. Prasad, D. Mehta, H.M. Azamathulla, N. Muttil, U. Rathnayake, Simulating the hydrological processes under multiple land use/land cover and climate change scenarios in the Mahanadi Reservoir complex, Chhattisgarh, India, Water 15 (2023) 3068, https://doi.org/10.3390/w15173068.
[25] S.M. Shravan Kumar, M. Pandey, A.K. Shukla, Spatio-temporal analysis of riverbank changes using remote sensing and geographic information system, Phys. Chem. Earth, Parts A/B/C 136 (2024) 103692, https://doi.org/10.1016/j.pce.2024.103692.
[26] K.H. Jodhani, H. Patel, U. Soni, R. Patel, B. Valodara, N. Gupta, A. Patel, P. jee Omar, Assessment of forest fire severity and land surface temperature using Google Earth Engine: a case study of Gujarat State, India, Fire Ecology 20 (2024) 23, https://doi.org/10.1186/s42408-024-00254-2.
[27] K.H. Jodhani, N. Gupta, A.D. Parmar, J.D. Bhavsar, H. Patel, D. Patel, S.K. Singh, U. Mishra, P. jee Omar, Synergizing google earth engine and earth observations for potential impact of land use/land cover on air quality, Results in Engineering 22 (2024) 102039, https://doi.org/10.1016/j.rineng.2024.102039.
[28] K.H. Jodhani, N. Gupta, A.D. Parmar, J.D. Bhavsar, D. Patel, S.K. Singh, U. Mishra, P.J. Omar, G.J. Omar, Unveiling seasonal fluctuations in air quality using google earth engine: a case study for Gujarat, India, Top. Catal. (2024), https://doi.org/10.1007/s11244-024-01957-1.
[29] H. Kumar, S.K. Karwariya, R. Kumar, Google earth engine-based identification of flood extent and flood-affected paddy rice fields using sentinel-2 MSI and sentinel-1 SAR data in Bihar state, India, Journal of the Indian Society of Remote Sensing 50 (2022) 791–803, https://doi.org/10.1007/s12524-021-01487-3.
[30] A.C. Pandey, K. Kaushik, B.R. Parida, Google earth engine for large-scale flood mapping using SAR data and impact assessment on agriculture and population of ganga-brahmaputra basin, Sustainability 14 (2022) 4210, https://doi.org/10.3390/su14074210.
[31] H. Mai Sy, C. Luu, Q.D. Bui, H. Ha, D.Q. Nguyen, Urban flood risk assessment using Sentinel-1 on the google earth engine: a case study in Thai Nguyen city, Vietnam, Remote Sens. Appl.: Society and Environment 31 (2023) 100987, https://doi.org/10.1016/j.rsase.2023.100987.
[32] M.R. Madadi, H.M. Azamathulla, M. Yakhkeshi, Application of Google earth to investigate the change of flood inundation area due to flood detention dam, Earth Science Informatics 8 (2015) 627–638, https://doi.org/10.1007/s12145-014-0197-8.
[33] D.P. Patel, P.K. Srivastava, M. Gupta, N. Nandhakumar, Decision Support System integrated with Geographic Information System to target restoration actions in watersheds of arid environment: a case study of Hathmati watershed, Sabarkantha district, Gujarat, J. Earth Syst. Sci. 124 (2015) 71–86, https://doi.org/10.1007/s12040-014-0515-z.
[34] R. Kumar Pradhan, P.K. Srivastava, S. Maurya, S. Kumar Singh, D.P. Patel, Integrated framework for soil and water conservation in Kosi River Basin, Geocarto Int. 35 (2020) 391–410, https://doi.org/10.1080/10106049.2018.1520921.
[35] R. Sinha, G.V. Bapalu, L.K. Singh, B. Rath, Flood risk analysis in the Kosi river basin, north Bihar using multi-parametric approach of Analytical Hierarchy Process (AHP), Journal of the Indian Society of Remote Sensing 36 (2008) 335–349, https://doi.org/10.1007/s12524-008-0034-y.
[36] Y.-R. Chen, C.-H. Yeh, B. Yu, Integrated application of the analytic hierarchy process and the geographic information system for flood risk assessment and flood plain management in Taiwan, Nat. Hazards 59 (2011) 1261–1276, https://doi.org/10.1007/s11069-011-9831-7.
[37] A. Malik, A. Kumar, H. Kandpal, Morphometric analysis and prioritization of sub-watersheds in a hilly watershed using weighted sum approach, Arabian J. Geosci. 12 (2019) 118, https://doi.org/10.1007/s12517-019-4310-7.
[38] O. Singh, D. Kumar, Evaluating the influence of watershed characteristics on flood vulnerability of Markanda River basin in north-west India, Nat. Hazards 96 (2019) 247–268, https://doi.org/10.1007/s11069-018-3540-4.
[39] F. Franci, G. Bitelli, E. Mandanici, D. Hadjimitsis, A. Agapiou, Satellite remote sensing and GIS-based multi-criteria analysis for flood hazard mapping, Nat. Hazards 83 (2016) 31–51, https://doi.org/10.1007/s11069-016-2504-9.
[40] V. Kumar, H. Md Azamathulla, K.V. Sharma, D.J. Mehta, K.T. Maharaj, The state of the art in deep learning applications, challenges, and future prospects: a comprehensive review of flood forecasting and management, Sustainability 15 (2023) 10543, https://doi.org/10.3390/su151310543.
[41] A. Abdelkarim, S.S. Al-Alola, H.M. Alogayell, S.A. Mohamed, I.I. Alkadi, I.Y. Ismail, Integration of GIS-based multicriteria decision analysis and analytic hierarchy process to assess flood hazard on the Al-shamal train pathway in Al-Qurayyat region, Kingdom of Saudi Arabia, Water 12 (2020) 1702, https://doi.org/10.3390/w12061702.
[42] S. Chakraborty, S. Mukhopadhyay, Assessing flood risk using analytical hierarchy process (AHP) and geographical information system (GIS): application in Coochbehar district of West Bengal, India, Nat. Hazards 99 (2019) 247–274, https://doi.org/10.1007/s11069-019-03737-7.
[43] A.A. Ameri, H.R. Pourghasemi, A. Cerda, Erodibility prioritization of sub-watersheds using morphometric parameters analysis and its mapping: a comparison among TOPSIS, VIKOR, SAW, and CF multi-criteria decision making models, Sci. Total Environ. 613–614 (2018) 1385–1400, https://doi.org/10.1016/j.scitotenv.2017.09.210.
[44] A. Patel, M.M. Singh, S.K. Singh, K. Kushwaha, R. Singh, AHP and TOPSIS based sub-watershed prioritization and Tectonic analysis of ami River Basin, Uttar Pradesh, J. Geol. Soc. India 98 (2022) 423–430, https://doi.org/10.1007/s12594-022-1995-0.
[45] M.R. Kafle, N.M. Shakya, Multi-criteria decision making approach for flood risk and sediment management in Koshi Alluvial fan, Nepal, J. Water Resour. Protect. 10 (2018) 596–619, https://doi.org/10.4236/jwarp.2018.106034.
[46] M. Karamouz, M. Taheri, P. Khalili, X. Chen, Building infrastructure resilience in Coastal flood risk management, J. Water Resour. Plann. Manag. 145 (2019), https://doi.org/10.1061/(ASCE)WR.1943-5452.0001043.
[47] S. Guguloth, M. Pandey, M. Pal, Application of Hybrid AI models for accurate prediction of Scour depths under submerged circular vertical jet, J. Hydrol. Eng. 29 (2024), https://doi.org/10.1061/JHYEFF.HEENG-6149.
[48] M. Pandey, M. Jamei, I. Ahmadianfar, M. Karbasi, A.S. Lodhi, X. Chu, Assessment of scouring around spur dike in cohesive sediment mixtures: a comparative study on three rigorous machine learning models, J. Hydrol. 606 (2022) 127330, https://doi.org/10.1016/j.jhydrol.2021.127330.
[49] S.K. Gupta, N. Gupta, V.P. Singh, Variable-sized cluster analysis for 3D pattern characterization of trends in precipitation and change-point detection, J. Hydrol. Eng. 26 (2021), https://doi.org/10.1061/(ASCE)HE.1943-5584.0002010.
[50] K.H. Jodhani, D. Patel, N. Madhavan, S.K. Singh, Soil erosion assessment by RUSLE, google earth engine, and geospatial techniques over Rel River Watershed, Gujarat, India, Water Conservation Science and Engineering 8 (2023) 49, https://doi.org/10.1007/s41101-023-00223-x.
[51] B. Ghosh, S. Mukhopadhyay, Erosion susceptibility mapping of sub-watersheds for management prioritization using MCDM-based ensemble approach, Arabian J. Geosci. 14 (2021) 36, https://doi.org/10.1007/s12517-020-06297-4.
[52] M.S. Tehrany, B. Pradhan, M.N. Jebur, Spatial prediction of flood susceptible areas using rule based decision tree (DT) and a novel ensemble bivariate and multivariate statistical models in GIS, J. Hydrol. 504 (2013) 69–79, https://doi.org/10.1016/j.jhydrol.2013.09.034.
[53] M.S. Tehrany, B. Pradhan, M.N. Jebur, Flood susceptibility mapping using a novel ensemble weights-of-evidence and support vector machine models in GIS, J. Hydrol. 512 (2014) 332–343, https://doi.org/10.1016/j.jhydrol.2014.03.008.
[54] B. Halder, S. Barman, P. Banik, P. Das, J. Bandyopadhyay, F. Tangang, S. Shahid, C. B. Pande, B. Al-Ramadan, Z.M. Yaseen, Large-scale flood hazard monitoring and impact assessment on landscape: representative case study in India, Sustainability 15 (2023) 11413, https://doi.org/10.3390/su151411413.